

OTTO-VON-GUERICKE-UNIVERSITÄT MAGDEBURG



**NUMERICAL MODELLING OF EQUILIBRIUM CAPILLARY
SURFACES: SOME METHODS AND RESULTS**

Viktor K. Polevikov

Computational Mathematics Department
Belarusian State University
Minsk 220050, Belarus
E-mail: polevikov@fpm.bsu.unibel.by

Preprint Nr. 10
1998

Fakultät für Mathematik

Impressum:

Herausgeber:

Otto-von-Guericke-Universität Magdeburg
Fakultät für Mathematik
Der Dekan

V. i. S. d. P.:

Lutz Tobiska
Postfach 4120
39016 Magdeburg

Preprint - sämtliche Rechte verbleiben den Autoren

Auflage: 150

Redaktionsschluß: März 1998

Redaktion/Gestaltung: Abt. Publikationen und Öffentlichkeitsarbeit

Herstellung: Dezernat Allgemeine Angelegenheiten,
Sachgebiet Reproduktion

NUMERICAL MODELLING OF EQUILIBRIUM CAPILLARY SURFACES: SOME METHODS AND RESULTS*

Viktor K. Polevikov

*Computational Mathematics Department
Belarusian State University
4 F. Skaryna Ave., Minsk 220050, Belarus
E-mail: polevikov@fpm.bsu.unibel.by*

Abstract. A new iteration-difference approach is proposed for numerical solving flat and axisymmetric problems on equilibrium shapes of a capillary surface called the tangential method or the T-method in virtue of constructional features. This method possesses a high order of approximation on a nonuniform grid, simple algorithm, improved agreement between an iteration solution and an exact solution of a differential problem. A condition for iteration convergence is obtained within the framework of a linear theory. As a result of tests, it is revealed that the proposed method is more economic as against other iteration-difference schemes and much exceeds them in computational stability. It is found that it adequately responds to physical collapse of equilibrium shapes, i. e. it can be adopted to investigate stability of equilibrium states of a capillary surface.

INTRODUCTION

Interest increased for the last 25—30 years in the study of equilibrium states of capillary liquid is mainly conditioned by applications occurred in space technology and hydromechanics of magneto- and electroconducting liquids. Just as the majority of practically important problems with a free boundary, the problems on equilibrium shapes of a capillary surface, as a rule, have a complex nonlinear statement. In the general case, we are dealing with the thermohydrodynamic problem, whose unknown solution is being sought in the domain with a preliminarily unknown boundary that is determined by an unknown solution. Exhaustive reviews of the theoretical methods for investigation of equilibrium capillary surfaces are presented in [1, 2]. These reviews show that methods for numerical modelling of doubly-connected, disconnected as well as simply-connected strongly curved surfaces in essence are not developed in modern computational hydrodynamics. The field of application of the existing approaches is limited mainly by problems with a simply-connected slightly curved surface.

In [3—6], the iteration-difference approach is developed. In [2], it is presented as a “rather universal because it is suitable for constructing equally both axisymmetric simply- and doubly-connected equilibrium surfaces and cylindrical ones (flat problem)”. Also, it

* Research has been partly supported by DFG grant EN 278/2-1.

should be added that it is efficient in the case of strongly curved surfaces and is easily extended to the class of disconnected surfaces.

The present work proposes a new method for computation of capillary surfaces. In virtue of constructional features, it is called the tangential method or the T-method. This method is shown to be more economic and much less sensitive to surface deformation in high fields as against the previous approaches. It can also serve for investigation of an equilibrium state as it adequately responds to a physical crisis of equilibrium shapes.

PARAMETRIC FREE SURFACE EQUATIONS

General equations. Consider an equilibrium capillary surface Γ of a viscous incompressible magnetic fluid (MF) that contacts a nonmagnetic gas medium and is acted on by gravitational and magnetic forces \mathbf{f} . Steady-state motion of such a fluid both inside a volume and on a free surface is governed by the equations:

$$\nabla p = -\rho(\mathbf{v} \cdot \nabla)\mathbf{v} + \eta \nabla^2 \mathbf{v} + \mathbf{f}, \quad \mathbf{f} = \rho \mathbf{g} + \mu_0 M \nabla H; \quad \nabla \cdot \mathbf{v} = 0 \quad (1)$$

where p is the fluid pressure; ρ the density; \mathbf{v} the velocity vector; $\eta = \text{const}$ the dynamic viscosity; \mathbf{g} the acceleration of gravity; μ_0 the magnetic constant; $M = M(H, \theta)$ the fluid magnetization; H the magnetic field intensity; θ the temperature. The isothermal fluid density ρ is assumed constant. In the case of nonisothermal fluid density, use is made of Boussinesque's approximation, taking into account the dependence $\rho(\theta)$ only in the right term \mathbf{f} .

Boundary conditions on the free surface are obtained from the general balance equations for normal and shear stresses with regard to capillary and magnetic pressure jump. If viscous stresses are neglected in the external (gas) medium, then the balance equation for normal stresses on the surface Γ assumes the form

$$p - p_0 = \sigma K - \frac{1}{2} \mu_0 \left(M \frac{H_n}{H} \right)^2 + 2\eta \frac{\partial v_n}{\partial n} \quad (2)$$

where $p_0 = \text{const}$ is the external pressure; σ the surface tension coefficient; K the sum of principal surface curvatures that takes a positive value if the surface is convex; H_n and v_n the normal vector components of magnetic intensity and velocity ($v_n = 0$ on the equilibrium surface).

Axisymmetric surface. If Γ is the surface of revolution, then its shape is determined by the equilibrium meridional line. Introduce the cylindrical coordinates R, Z by bringing the OZ axis into coincidence with the symmetry axis and by directing it opposite to the gravity vector. Let S be an arc length of an unknown equilibrium line that ranges from $S = 0$ to $S = l$. The equilibrium line shape will be described by the parametric functions $R(S), Z(S)$. Then $\mathbf{n} = (-Z', R')$, $\mathbf{t} = (R', Z')$ are the vectors of the normal and tangent to the equilibrium line in the R, Z plane (prime means differentiation with respect to S). Note that the tangent vector \mathbf{t} is oriented in the direction of increasing S . The surface curvature is calculated by the formula $K = \phi(RZ')' / (RR')$ where we choose $\phi = -1$ if while moving along the

equilibrium line in the direction of increasing S fluid remains on the right, and $\phi = 1$ if fluid remains on the left.

By means of simple manipulations with Eq. (1) with regard to the equilibrium condition $v_n = \mathbf{v} \cdot \mathbf{n} = 0$, on the surface Γ we have

$$\frac{\partial p}{\partial S} = \nabla p \cdot \mathbf{t} = -\frac{1}{2}\rho \frac{\partial(v_s^2)}{\partial S} + \rho \frac{R'}{R} v_\phi^2 - \eta \frac{1}{R} \frac{\partial(Rw)}{\partial n} - \rho g Z' + \mu_0 \frac{\partial}{\partial S} \int_0^H M dH$$

where v_s and v_ϕ are the tangential and azimuthal velocity components, and

$$w = \frac{\partial v_z}{\partial R} - \frac{\partial v_R}{\partial Z}$$

is the vorticity. Hence, for any point $R(S)$, $Z(S)$ of the free surface we find

$$p = \Pi + \text{const}, \quad (3)$$

$$\Pi = -\frac{1}{2}\rho v_s^2 + \int_0^S \left(\rho \frac{R'}{R} v_\phi^2 - \eta \frac{1}{R} \frac{\partial(Rw)}{\partial n} - \rho g Z' \right) dS + \mu_0 \int_0^H M dH$$

By eliminating the pressure p from Eqs (2), (3), we obtain a parametric differential equation for the axisymmetric surface Γ

$$Z'' = R'F; \quad 0 < S < l \quad (4)$$

where

$$F = \phi \Psi / \sigma + \text{const} - \frac{Z'}{R}, \quad \Psi = \Pi + \frac{1}{2}\mu_0 \left(M \frac{H_n}{H} \right)^2 - 2\eta \frac{\partial v_n}{\partial n}.$$

The natural condition $R'^2 + Z'^2 = 1$ serves as one more equation. By using differentiation, it can be replaced by $R'' = -Z'F$. For the natural condition in this case not to be violated, it should be satisfied, at least, at one value of S , e. g. at $S = 0$ or $S = l$.

Cylindrical surface (flat problem). In the case of the flat problem, a cylindrical equilibrium surface is determined by the equilibrium line of cross-section. Introduce into the cross-section plane the Cartesian coordinates X, Y by directing the OY axis opposite to the vector \mathbf{g} . In these coordinates $K = \phi Y'' / X' = -\phi X'' / Y'$ where $X = X(S)$ and $Y = Y(S)$ are the unknown parametric functions describing the shape of the equilibrium line. By analogy with the axisymmetric case, we arrive at the equations

$$Y'' = X'F, \quad X'' = -Y'F; \quad 0 < S < l;$$

$$F = \phi \Psi / \sigma + \text{const}, \quad \Psi = \Pi + \frac{1}{2}\mu_0 \left(M \frac{H_n}{H} \right)^2 - 2\eta \frac{\partial v_n}{\partial n},$$

$$\Pi = -\frac{1}{2}\rho v_s^2 + \int_0^S \left(-\eta \frac{\partial w}{\partial n} - \rho g Y' \right) dS + \mu_0 \int_0^H M dH, \quad w = \frac{\partial v_y}{\partial X} - \frac{\partial v_x}{\partial Y}$$

whose solution requires the condition $X'^2 + Y'^2 = 1$ to be satisfied.

The obtained differential equations are supplemented with the boundary conditions of the first and second kinds as well as with the non-local (integral) condition of fluid volume conservation. By boundary conditions can be understood either conditions when fluid contacts a solid wall specified by wall geometry and an assigned wetting angle, or symmetry conditions.

TEST PROBLEMS

To test algorithms two hydrostatics problems on axially symmetric equilibrium shapes of a simply-connected capillary surface were chosen. These are:

- (1) problem on a drop adjacent to a horizontal rotating plate in a gravity field;
- (2) problem on an isolated MF drop in a high uniform magnetic field.

The first of them is the classical problem of capillary hydrostatics [1, 2, 5, 7] and the second is the known problem of MF statics [3, 6, 8, 9].

Problem 1. Place the origin of coordinates on the plate surface, namely, in the middle of the drop base, and let an arc length take a value $S = 0$ at the drop apex (i. e. at $R = 0$) and $S = l$ at the point where the meridian contacts the plane $Z = 0$. Since the magnetic forces are absent in equation (4), we have $\Psi = \Pi = -\rho g [Z - Z(0)] + \rho \omega^2 R^2 / 2$ where ω is the angular rotation velocity of a drop. So, the equations for a drop surface are obtained as

$$R'' = -Z'F, \quad Z'' = R'F; \quad F = \phi \left(-\frac{\rho g}{\sigma} Z + \frac{\rho \omega^2}{2\sigma} R^2 \right) - \frac{Z'}{R} + \text{const}; \quad 0 < S < l \quad (5)$$

Boundary conditions follow from the symmetry conditions at $S = 0$ and from the conditions when fluid contacts the solid wall at $S = l$:

$$R(0) = 0, \quad R'(0) = 1, \quad Z'(0) = 0; \quad Z(l) = 0, \quad R(l) = \cos \alpha, \quad Z'(l) = \phi \sin \alpha \quad (6)$$

where α is the wetting (contact) angle. Assuming that the drop volume V is assigned, it can be determined as a volume of a body of revolution:

$$V = -2\pi \phi \int_0^l Z R R' dS \quad (7)$$

Thus, the mathematical statement of the problem for $R(S)$ and $Z(S)$ consists of differential Eqs (5), boundary conditions (6), and integral condition (7). The adopted direction of increasing S owes us to choose $\phi = -1$ if a drop is adjacent to the plate from above (sessile drop) and $\phi = 1$ if a drop is adjacent to the plate from below (pendent drop).

Problem 2. Consider an MF drop not contacting a solid wall and acted on by a high uniform magnetic field under zero-gravity in the state of magnetic saturation. Assume that the vector of the field intensity is collinear to the OZ symmetry axis. Then $\mathbf{f} = \mu_0 \vec{M} \nabla H = 0$, $H_n = \pm H R'$ and it should be obviously assumed in Eq. (4) that $\Psi = \mu_0 \vec{M}^2 R'^2 / 2$ where \vec{M} is the fluid saturation magnetization. Considering that a drop is symmetric relative to the equatorial plane $Z = 0$, we restrict ourselves to the half-space $Z \geq 0$. As in Problem 1, choose the point $S = 0$ on the OZ axis and the point $S = l$, on the plane $Z = 0$. The choice is consistent with $\phi = -1$. Hence, the drop shape is described by the equations

$$R'' = -Z'F, \quad Z'' = R'F; \quad F = -\frac{\mu_0 \vec{M}^2}{2\sigma} R'^2 - \frac{Z'}{R} + \text{const}; \quad 0 < S < l \quad (8)$$

Boundary conditions are formulated with regard to the drop symmetry:

$$R(0) = Z'(0) = Z(l) = R'(l) = 0, \quad R'(0) = 1, \quad Z'(l) = -1 \quad (9)$$

The mathematical model is closed by an expression that relates the solution to the drop volume V :

$$V = 4\pi \int_0^l Z R R' dS \quad (10)$$

CHANGE OF VARIABLES

The specific feature of the parametric statement is that the length, l , of the equilibrium line, i. e. the domain of definition of the problem, is beforehand unknown. This causes great difficulties for numerical solving. A procedure of nondimensionalizing is an important element for constructing algorithms of the iteration-difference approach. This procedure allows us to move the unknown length into the equations and make computations on a fixed interval $[0, 1]$.

Choose l as a characteristic dimension and introduce dimensionless variables

$$s = S/l, \quad r = R/l, \quad z = Z/l \quad (11)$$

Problem 1. In new variables, problem (5)—(7) takes the form:

$$r'' = -z'(f + C), \quad z'' = r'(f + C); \quad (12)$$

$$f = \phi(-\text{Bo}L^2 z + \text{PL}^3 r^2) - z'/r; \quad 0 < s < 1;$$

$$r(0) = 0, \quad r'(0) = 1, \quad z'(0) = 0, \quad (13)$$

$$z(1) = 0, \quad r'(1) = \cos(\phi\alpha), \quad z'(1) = \sin(\phi\alpha);$$

$$L = \left(-2\pi\phi \int_0^1 z r r' ds \right)^{-1/3} \quad (14)$$

where $Bo = \rho g V^{2/3} / \sigma$ is the Bond number that characterizes the gravitational-to-capillary force ratio; $P = \rho \omega^2 V / (2\sigma)$ is the parameter having a meaning of the centrifugal-to-capillary force ratio; $L = l / V^{1/3}$; C is the constant not yet defined. To define the constant C , write down one of Eqs (12) as $(r z')' = r r' [\phi(-Bo L^2 z + P L^3 r^2) + C]$. Then having integrated it on the interval $[0, 1]$ with regard to conditions (13) and (14), we obtain:

$$C = \phi \left(\frac{2 \sin \alpha}{r(1)} - \frac{1}{2} P L^3 r^2(1) \right) - \frac{Bo}{\pi L r^2(1)}. \quad (15)$$

Problem 2. Now formulate problem (8)—(10) in new variables:

$$r'' = -z'(f + C), \quad z'' = r'(f + C); \quad f = -W L r'^2 - \frac{z'}{r}; \quad 0 < s < 1; \quad (16)$$

$$r(0) = 0, \quad r'(0) = 1, \quad z'(0) = 0, \quad z(1) = 0, \quad r'(1) = 0, \quad z'(1) = -1; \quad (17)$$

$$L = \left(4\pi \int_0^1 z r r' ds \right)^{-1/3} = \left(-2\pi \int_0^1 z' r^2 ds \right)^{-1/3} \quad (18)$$

where $W = \mu_0 M^2 V^{1/3} / (2\sigma)$ is the dimensionless parameter that characterizes the ratio of a magnetic pressure jump on a free surface to a capillary jump; $L = l / V^{1/3}$. The dependence of the constant C on a solution is defined similarly as in Problem 1:

$$C = \frac{2}{r^2(1)} \left(-r(1) + W L \int_0^1 r r'^3 ds \right). \quad (19)$$

It should be noted that the main objective to use change of variables (11) is that we want to obtain an explicit stable formula for correction of the dimensionless length L while solving the nonlinear problem on free surface equilibrium in iterations. This is achieved by the integral condition that in Problems 1 and 2 reduces to (14) and (18), respectively, and is convenient for recalculation of the length L in each iteration of the algorithm of successive refinement of an unknown boundary.

Since in the algorithm of the iteration-difference method we seek for the solution $r(s)$, $z(s)$ that obeys the unit length of the equilibrium line of the free surface but not the assigned fluid volume, as the initial statement of the problem requires, usually the variables $\tilde{r} = R / V^{1/3}$, $\tilde{z} = Z / V^{1/3}$ nondimensionalized by the volume V are used to analyze the result obtained. A transition from variables (11) to them is made by simple recalculation: $\tilde{r} = r \cdot L$, $\tilde{z} = z \cdot L$.

ITERATION-DIFFERENCE SCHEMES

Let us formulate a two-dimensional problem on the equilibrium shape of a capillary surface in the following general form:

$$x'' + y' F = 0, \quad y'' - x' F = 0; \quad 0 < s < 1; \quad (20)$$

$$x(0) = a_0, \quad y(1) = b_1, \quad (21)$$

$$x'(0) = \cos \gamma_0, \quad y'(0) = \sin \gamma_0, \quad x'(1) = \cos \gamma_1, \quad y'(1) = \sin \gamma_1$$

where $x(s)$ and $y(s)$ are the unknown parametric functions; $F = f + C$; $f = f(x, y, x', y', L)$ is the assigned function; C and L are the constants being the functionals of the known form of the solution; $a_0, \gamma_0, b_1, \gamma_1$ are the predetermined constants. Expressions for f and C can also contain functions of solution, whose analytical form is unknown but their numerical values are determined by solving some additional problem, e. g. problem on a magnetic field distribution or a hydrodynamic process in an MF volume. In the case of the flat problem, appearing here x and y are the dimensionless Cartesian coordinates of a surface, and in the case of the axisymmetric problem by them are understood the cylindrical coordinates r, z .

The identity $x'^2 + y'^2 \equiv 1$ is the natural property of the parametric equations $x(s), y(s)$. From system (20) it can be easily obtained that if this equality is obeyed at some one value of s , then it is also valid for all $s \in [0, 1]$. In virtue of this, when problem (20), (21) is solved, any of the last four conditions of (21) can be neglected. In addition, one of the remaining three conditions was formally needed to define the dependence of the constant C on a solution.

Let us construct a difference scheme of the second-order approximation on the uniform grid $\{s_i = i \cdot h \mid i = 0, 1, K, N; h = 1/N\}$ for problem (20), (21) by designating a difference solution by the same letters as the exact solution:

$$\begin{aligned} \Lambda_1(x, y, F)|_i &\equiv x_{\bar{s}, i} + y_{s, i} F_i = 0, \\ \Lambda_2(x, y, F)|_i &\equiv y_{\bar{s}, i} - x_{s, i} F_i = 0; \quad i = \overline{1, N-1}; \end{aligned} \quad (22)$$

$$x_0 = a_0, \quad x_{\bar{s}, N} = \cos \gamma_1 + \frac{h}{2} F_N \sin \gamma_1;$$

$$y_{s, 0} = \sin \gamma_0 + \frac{h}{2} F_0 \cos \gamma_0, \quad y_N = b_1$$

where

$$F_i = f_i + C, \quad f_i = f(x_i, y_i, x_{s,i}^o, y_{s,i}^o, L), \quad i = \overline{1, N-1};$$

$$f_0 = f(a_0, y_0, \cos \gamma_0, \sin \gamma_0, L); \quad f_N = f(x_N, b_1, \cos \gamma_1, \sin \gamma_1, L);$$

$$x_{s,i} = (x_{i+1} - x_i) / h, \quad x_{\bar{s},i} = (x_i - x_{i-1}) / h,$$

$$x_{s,i}^o = (x_{i+1} - x_{i-1}) / (2h), \quad x_{\bar{s},i}^o = (x_{s,i} - x_{\bar{s},i}) / h.$$

To solve nonlinear difference problem (22), consider two two-layer iteration schemes:

$$\frac{1}{\tau}(x_{\bar{s},i}^{n+1} - x_{\bar{s},i}^n) + \Lambda_1(x^n, y^n, F^n)|_i = 0, \quad i = \overline{1, N-1}, \quad (23)$$

$$x_0^{n+1} = a_0, \quad x_{\bar{s},N}^{n+1} = \cos \gamma_1 + \frac{h}{2} F_N^n \sin \gamma_1;$$

$$\frac{1}{\tau}(y_{\bar{s},i}^{n+1} - y_{\bar{s},i}^n) + \Lambda_2(x^n, y^n, F^n)|_i = 0, \quad i = \overline{1, N-1}, \quad (24)$$

$$y_{s,0}^{n+1} = \sin \gamma_0 + \frac{h}{2} F_0^n \cos \gamma_0, \quad y_N^{n+1} = b_1$$

and

$$\frac{x_i^{n+1} - x_i^n}{\tau} = x_{\bar{s},i}^{n+1} + y_{s,i}^n F_i^n, \quad i = \overline{1, N-1}; \quad (25)$$

$$x_0^{n+1} = a_0, \quad x_{\bar{s},N}^{n+1} = \cos \gamma_1 + \frac{h}{2} F_N^n \sin \gamma_1;$$

$$\frac{y_i^{n+1} - y_i^n}{\tau} = y_{\bar{s},i}^{n+1} - x_{s,i}^n F_i^n, \quad i = \overline{1, N-1}; \quad (26)$$

$$y_{s,0}^{n+1} = \sin \gamma_0 + \frac{h}{2} F_0^n \cos \gamma_0, \quad y_N^{n+1} = b_1$$

where $n = 0, 1, 2, K$ is the iteration number; $\tau > 0$ is the relaxation parameter; $F_i^n = f_i^n + C^n$; $f_i^n = f(x_i^n, y_i^n, x_{s,i}^n, y_{s,i}^n, L^n)$.

Both scheme (23), (24) and scheme (25), (26) are realized in each iteration by means of the elimination procedure applied to each of problems (23)—(26). As a result, new iteration approximations x^{n+1} and y^{n+1} are determined.

Scheme (23), (24) was successfully used to compute equilibrium shapes of simply connected [3, 6] and doubly-connected [4, 10—12] surfaces both in the presence of gravitational, centrifugal and magnetic forces and in their absence under zero-gravity. By

using this scheme, we managed for the first time to numerically solve the problem of capillary hydrostatics with an essentially disconnected free surface, namely, the problem on equilibrium states of a magnetic fluid seal when acted on by an external pressure drop [13]. Scheme (25), (26) was adopted to investigate equilibrium states of a drop rotating in a gravitational field [5].

TANGENTIAL METHOD (T-METHOD)

Introduce into our consideration a new unknown $\beta(s)$ being an angle between the tangent to the equilibrium line $x(s)$, $y(s)$ and the Ox axis. Bearing in mind that $x' = \cos\beta$, $y' = \sin\beta$, problem (20), (21) can be reformulated as

$$\begin{aligned}\beta' &= F, \quad \beta(0) = \gamma_0, \quad \beta(1) = \gamma_1; \\ x' &= \cos\beta, \quad x(0) = a_0; \\ y' &= \sin\beta, \quad y(1) = b_1.\end{aligned}\tag{27}$$

In such a statement, the identity $x'^2 + y'^2 \equiv 1$ is satisfied irrespective of boundary conditions. Assuming that the conditions $\beta(0) = \gamma_0$ and $\beta(1) = \gamma_1$ have been already used to describe the constant C , it is enough to leave only one of them in problem (27).

On the nonuniform grid $\{s_i = s_{i-1} + h_i \mid i = 1, 2, K, N; s_0 = 0, s_N = 1\}$ for problem (27) we shall consider a difference scheme of the fourth-order approximation:

$$\begin{aligned}\frac{\beta_i - \beta_{i-1}}{h_i} &= \Phi_i, \quad \Phi_i = \frac{1}{2}(F_{i-1} + F_i) - \frac{1}{12}h_i(f'_i - f'_{i-1}); \\ \frac{x_i - x_{i-1}}{h_i} &= X(\beta, F)|_i, \quad X(\beta, F)|_i = \frac{1}{2}(u_{i-1} + u_i) + \frac{1}{12}h_i(F_i v_i - F_{i-1} v_{i-1}); \\ \frac{y_i - y_{i-1}}{h_i} &= Y(\beta, F)|_i, \quad Y(\beta, F)|_i = \frac{1}{2}(v_{i-1} + v_i) - \frac{1}{12}h_i(F_i u_i - F_{i-1} u_{i-1}); \\ i &= \overline{1, N}; \quad \beta_0 = \gamma_0, \quad \beta_N = \gamma_1; \quad x_0 = a_0; \quad y_N = b_1\end{aligned}\tag{28}$$

where

$$F = f + C, \quad f = f(x, y, u, v, L),$$

$$f' = \frac{\partial f}{\partial x}u + \frac{\partial f}{\partial y}v - \frac{\partial f}{\partial u}Fv + \frac{\partial f}{\partial v}Fu, \quad u = \cos\beta, \quad v = \sin\beta.$$

If in expressions for Φ_i, X_i, Y_i the h_i -containing addends are omitted, then the obtained system will be of the second-order approximation with respect to problem (27).

In view of (28), the iteration algorithm for computation of free surface coordinates will be constructed as

$$\beta_i^{n+1} = \beta_{i+1}^{n+1} - h_{i+1} \Phi_{i+1}^n + (1 - \tau)(\beta_i^n - \beta_{i+1}^n + h_{i+1} \Phi_{i+1}^n), \quad (29)$$

$$i = N - 1, N - 2, K, 1; \quad \beta_N^{n+1} = \gamma_1; \quad \beta_0^{n+1} = \gamma_0$$

$$x_i^{n+1} = x_{i-1}^{n+1} + h_i X(\beta^{n+1}, F^n)|_i, \quad i = 1, 2, K, N; \quad x_0^{n+1} = a_0 \quad (30)$$

$$y_i^{n+1} = y_{i+1}^{n+1} - h_{i+1} Y(\beta^{n+1}, F^n)|_{i+1}, \quad i = N - 1, N - 2, K, 0; \quad y_N^{n+1} = b_1 \quad (31)$$

Instead of (29), it is possible to use the following procedure

$$\beta_i^{n+1} = \beta_{i-1}^{n+1} + h_i \Phi_i^n + (1 - \tau)(\beta_i^n - \beta_{i-1}^n - h_i \Phi_i^n), \quad i = \overline{1, N - 1}; \quad (32)$$

$$\beta_0^{n+1} = \gamma_0; \quad \beta_N^{n+1} = \gamma_1.$$

Computations in each iteration are made by direct algorithms of running count. First, recurrence rules (29) or (32) are used to compute grid values of β_i^{n+1} . Then, by employing procedures (30) and (31), new iteration approximations are determined for free surface coordinates. And, at last, grid functions F_i^{n+1} and Φ_i^{n+1} are formed by the found values of $x_i^{n+1}, y_i^{n+1}, \beta_i^{n+1}$. The direction of passing through nodes in algorithms (30) and (31) obeys a particular statement of differential problem on a capillary surface shape. For other statements it can be otherwise, not changing the essence of the method.

The obvious advantages of the T-method are: high order of approximation on a nonuniform grid, exact approximation of boundary conditions, simple design, and simple realization of an algorithm. Unlike iteration-difference schemes (23), (24) and (25), (26), the T-method provides the difference analog of the condition $x'^2 + y'^2 = 1$ to be implemented at all nodes, in each iteration and at any τ . By doing so, the better agreement between the iteration solution and the exact solution of the differential problem is attained.

Computational stability. Assume that a computational error appears in the $(n + 1)$ -th iteration in the boundary conditions so that the conditions $\tilde{\beta}_N^{n+1} = \gamma_1 + \delta_N$, $\tilde{x}_0^{n+1} = a_0 + \xi_0$, $\tilde{y}_N^{n+1} = b_1 + \eta_N$ are in fact utilized in algorithms (29)–(31). When affected by small errors δ_N, ξ_0 and η_N in the $(n + 1)$ -th iteration, we obtain the following solution $\tilde{\beta}_i^{n+1} = \beta_i^{n+1} + \delta_i$, $\tilde{x}_i^{n+1} = x_i^{n+1} + \xi_i$, $\tilde{y}_i^{n+1} = y_i^{n+1} + \eta_i$; $i = \overline{0, N}$. Bearing in mind that the grid functions $\beta^{n+1}, x^{n+1}, y^{n+1}$ also obey Eqs (29)–(31) and by using simple trigonometric manipulations, we arrive at the following relations for a computational error at the grid nodes:

$$\delta_i = \delta_{i+1} = \delta_{i+2} = K = \delta_N; \quad i = \overline{1, N} \quad (33)$$

$$\xi_i = \xi_0 - \sum_{k=1}^i \left\{ h_k \left[\sin \frac{\delta_{k-1}}{2} \sin \left(\beta_{k-1}^{n+1} + \frac{\delta_{k-1}}{2} \right) + \sin \frac{\delta_k}{2} \sin \left(\beta_k^{n+1} + \frac{\delta_k}{2} \right) \right] + \right. \\ \left. + \frac{h_k^2}{6} \left[F_{k-1}^n \sin \frac{\delta_{k-1}}{2} \cos \left(\beta_{k-1}^{n+1} + \frac{\delta_{k-1}}{2} \right) - F_k^n \sin \frac{\delta_k}{2} \cos \left(\beta_k^{n+1} + \frac{\delta_k}{2} \right) \right] \right\}; \quad i = \overline{1, N} \quad (34)$$

$$\eta_i = \eta_N - \sum_{k=i+1}^N \left\{ h_k \left[\sin \frac{\delta_{k-1}}{2} \cos \left(\beta_{k-1}^{n+1} + \frac{\delta_{k-1}}{2} \right) + \sin \frac{\delta_k}{2} \cos \left(\beta_k^{n+1} + \frac{\delta_k}{2} \right) \right] + \right. \\ \left. + \frac{h_k^2}{6} \left[F_{k-1}^n \sin \frac{\delta_{k-1}}{2} \sin \left(\beta_{k-1}^{n+1} + \frac{\delta_{k-1}}{2} \right) - F_k^n \sin \frac{\delta_k}{2} \sin \left(\beta_k^{n+1} + \frac{\delta_k}{2} \right) \right] \right\}; \quad i = \overline{0, N-1} \quad (35)$$

Equalities (33) point to absolute stability of procedure (29). Based on relations (34) and (35) with regard to (33), it is easy to make the following rough estimates

$$|\xi_i| \leq |\xi_0| + |\delta_N| \left(1 + \frac{h_k}{6} \max_{1 \leq k \leq N} |F_k^n| \right), \\ |\eta_i| \leq |\eta_N| + |\delta_N| \left(1 + \frac{h_k}{6} \max_{1 \leq k \leq N} |F_k^n| \right); \quad i = \overline{0, N}.$$

They mean that procedures (30) and (31) are also stable. Hence, the algorithm for realization of the tangential method in each iteration is absolutely stable.

Convergence of iterations. Convergence of iteration process (29)—(31) as $n \rightarrow \infty$ can be investigated, assuming that the function F does not depend on a solution, i. e. $\Phi_i^n = \Phi_i$ at all $n = 0, 1, 2, K$. In this case, iterations are made only according to algorithm (29). Let β_i be an unknown difference solution. Designate the iteration error as $\varepsilon_i^n = \beta_i^n - \beta_i$; $i = 0, 1, K, N$; $n = 0, 1, 2, K$; where ε^0 is the initial iteration approximation. Assuming $\varepsilon_0^n = \varepsilon_N^n = 0$ and substituting $\beta^n = \beta + \varepsilon^n$ into (29) yields for the error the problem

$$\varepsilon_i^{n+1} - (1 - \tau)\varepsilon_i^n = \varepsilon_{i+1}^{n+1} - (1 - \tau)\varepsilon_{i+1}^n; \quad i = N-1, N-2, K, 1; \quad \varepsilon_N^{n+1} = 0$$

which is decomposed into a system of the equalities $\varepsilon_i^{n+1} - (1 - \tau)\varepsilon_i^n = 0$; $i = 1, 2, K, N-1$. Hence, the iteration error in the n -th iteration is related to the error of the initial approximation by $\varepsilon_i^n = (1 - \tau)\varepsilon_i^{n-1} = (1 - \tau)^2 \varepsilon_i^{n-2} = K = (1 - \tau)^n \varepsilon_i^0$; $i = \overline{0, N}$. From this it follows that the condition

$$0 < \tau < \tau^* = 2 \quad (36)$$

is necessary and sufficient for iteration convergence as $n \rightarrow \infty$.

Condition (36) is obtained to a linear approximation. Experience shows that as the nonlinearity grows, the convergence domain $(0, \tau^*)$ gradually narrows, tending to zero ($\tau^* \rightarrow 0$).

RESULTS OF TESTS

Iteration schemes were tested on problems (12)—(15) and (16)—(19). It is known that the existence of equilibrium states in Problem 1 is limited by small values of the rotation parameter $P < P_c(\alpha, Bo)$ and in the case of a pendent drop ($\phi = 1$) also of the Bond number $Bo < Bo_c(\alpha, P)$, at excess of which there occurs an equilibrium crisis. The choice of Problem 1 as a test one is explained by our wish to compare the critical values of Bo_c and P_c obtained by a sign of computational instability of iteration schemes with the known data of linear theory for stability of equilibrium capillary surfaces. It was assumed that a value of the Bond number or the parameter P exceeded a critical one if at this value iterations diverged. Critical values of Bo_c and P_c were refined by the dichotomy method unless their error became less than $\delta = 5 \cdot 10^{-4}$.

As for Problem 2, the mechanism of physical collapse of equilibrium shapes was revealed neither theoretically nor experimentally [8, 9]. As the parameter W grows, an MF drop is elongated along the field direction, not breaking. The surface curvature at the drop apexes $K(0)$ in this case increases and decreases near the equatorial line. Problem 2 is a good tool to test iteration schemes for "strength" since the onset of instability, when schemes are implemented, may be only computational in nature. It is found [6] that as the parameter W grows, the curvature $K(0)$ increases almost according to the linear law so that the influence of the parameter W on iteration convergence can be interpreted as the curvature influence.

Furthermore, for brevity, schemes (23), (24) and (25), (26) will be called the scheme A and the scheme B , respectively; the algorithm of the tangential method (29)—(31), the scheme T , and its variant of the second order of accuracy, the scheme $T-2$. Taking into account the statement of the test problems, in the algorithms A , B , T it was assumed that $x \sim r$, $y \sim z$; $a_0 = b_1 = \gamma_0 = 0$; $\gamma_1 = \phi\alpha$ for Problem 1 and $\gamma_1 = -\pi/2$ for Problem 2. Integrals in the constants L and C were approximated by the same order as the differential equations: the schemes A , B used the analog of the trapezoid rule and the scheme T , the Euler rule. So, e. g. in the case of a uniform grid the constants L and C in each iteration of the algorithm T were calculated by the formulas:

$$1) L = \left\{ -2\pi\phi \left[h \sum_{i=1}^{N-1} z_i r_i \cos \beta_i + \frac{h^2}{12} \left(z_0 - \phi \frac{r_N}{2} \sin 2\alpha \right) \right] \right\}^{-1/3},$$

$$C = \phi \left(\frac{2 \sin \alpha}{r_N} - PL^3 \frac{r_N^2}{2} \right) - \frac{Bo}{\pi L r_N^2};$$

$$2) L = \left[-2\pi h \left(\sum_{i=1}^{N-1} r_i^2 \sin \beta_i - \frac{1}{2} r_N^2 \right) \right]^{-1/3}, \quad C = \frac{2}{r_N^2} \left[-r_N + WL \left(h \sum_{i=1}^{N-1} r_i \cos^3 \beta_i + \frac{h^2}{12} \right) \right]$$

where the first two formulas refer to Problem 1 and two others, to Problem 2. The corresponding formulas for the scheme $T-2$ differ from the above mentioned by the absence of the addends containing h^2 .

As a criterion for accuracy of an iteration solution, consideration was made of a value of the discrepancy of the difference equations, i. e. the iterations A and B continued unless the condition $\max_{k=1,2} \|\Lambda_k(r^n, z^n, F^n)\|_C \leq \varepsilon$ was satisfied, and the iterations T continued unless the condition $\max_{0 < i < N} |(\beta_{i+1}^n - \beta_i^n) / h_{i+1} - \Phi_{i+1}^n| \leq \varepsilon$ was satisfied at any number $n = n(\varepsilon)$; where the operators Λ_k were of form (22). Calculations were made with an iteration error $\varepsilon = 10^{-4}$ on uniform grids with the steps $h = 1/100$ and $1/20$ as well as on an adaptive grid with the number of partitions $N = 100$. Nodes of the adaptive grid were generated by the a priori method described in [6].

As calculations showed, because of simplification of running count procedures and reduction of their number, when going from one iteration to another, the scheme T spent for one iteration a machine time that was 1.5—2 time less than the one spent by the schemes A and B .

Problem 1. Comparison with the theory [1, 2] has shown that a crisis of the computational process occurs at the same Bo_c and P_c as a collapse of equilibrium shapes. So, for an immovable pendent drop ($P = 0$, $\phi = 1$) at $\alpha = 45^\circ$ the theoretical value is $Bo_c = 4.988$ and we have numerically obtained $Bo_c = 4.982$ at $h = 1/100$ by using the scheme A ; at $\alpha = 135^\circ$ these values have appeared to be 0.579 and 0.580, respectively, and at $\alpha = 90^\circ$, 2.265 and 2.265. It should be said that the presented data of stability theory were calculated by means of interpolation of Table 9 from [2], with the use of a cubic spline determined on a pattern of 4 nodes: two on the left and two on the right of a value of α chosen for comparison. To avoid the influence of an interpolation error the angle $\alpha = 1.523$ was considered in more detail. The above table contains an exact value $Bo_c = 2.407$ obtained by the analytical methods for this angle. As a result of numerical experiment at $h = 1/20$, critical values $Bo_c = 2.3970 \pm \delta$ (schemes A and B), $2.4185 \pm \delta$ (scheme $T-2$), $2.4058 \pm \delta$ (scheme T) were obtained. At $h = 1/100$ all schemes showed the same result $Bo_c = 2.4058 \pm \delta$. An unremovable 0.001 difference between the analytical and numerical values of Bo_c can be caused by an error of linear theory which occurs due to a neglect of second-order infinitesimal disturbances.

Theoretically, equilibrium stability of a rotating drop is studied only at $Bo = 0$, $\alpha = 90^\circ$. A critical value of the rotation parameter $P_c = 4.7613 \pm \delta$ found numerically at $h = 1/100$ in fact does not differ from a theoretical one $P_c = 4.763$ [2].

The equally exact coincidence of the theoretical and numerical values of the critical parameters was observed in [12, 13] in the problem on MF seal stability, for whose solution the scheme A was used, as well as in other problems. Thus, as a result of numerical experiment it is found that all presented iteration algorithms adequately respond to a crisis of the equilibrium state of a free surface: if at some values of the problem parameters equilibrium shapes collapse due to flat or axisymmetric disturbances, then computational instability appears at the same critical values.

Problem 2. Comparison of the algorithms A , B , T by the most important convergence indices of the iteration process was made mainly in Problem 2. Table 1 comprises the data on convergence rate and computational stability when W grows. The left columns at each τ correspond to the scheme A ; the middle ones, to the scheme B ; the right ones, to the scheme T ; the crosses stand for divergence of the iteration process. The exhaustion of the W values was made at a step of 2.5. For each new variant, the solution obtained for the previous W served as an initial iteration approximation. The initial approximation for $W = 2.5$ is an exact

solution at $W=0$. As we see, the scheme T does not concede the schemes A and B in convergence rate but much exceeds them in stability.

Let us emphasize the inconsistency of the scheme B in the case of strongly curved (locally disturbed) surfaces characteristic for magnetizing and electrically conducting fluids in high fields. Indeed, the stability domain of the scheme B is limited by the value $W \approx 15$, at which the curvature $K(0)$ only 5.5 times exceeds the curvature, K_0 , of a spherical drop at $W=0$. For comparison: at $W=150$ limiting for the scheme T at $h=1/100$ the relative curvature attains $K(0)/K_0 = 47.6$. At the same time, when capillary surfaces are calculated in a gravitational field, the scheme B can be rather efficient [5]. In this case, a maximum value of the curvature K as a rule does not much differ from the spherical surface curvature that is realized under zero-gravity, and physical instability occurs earlier than computational one.

Fig. 1 plots the boundaries of computational stability of iteration schemes. Each curve divides the domain (W, τ) into two subdomains: computational stability domain lies below the curve while the computational instability one, above it. It is seen that both schemes of tangential method (T and $T-2$) are stable over an essentially wider range of parameters than the schemes A and B . Note that the stability domain of the scheme B does not depend on the step h , the stability of the remaining schemes is much improved as h decreases.

Adaptive grid. An adaptive grid has proved to be a powerful tool to stabilize iterations as the surface curvature grows. If on the uniform grid with the step $h=1/100$ the stability domain of the scheme T is limited by the value $W \approx 150$ (see Table 1), then on the adaptive grid the stability boundary moves to $W=4800$. Because of an optimal distribution of the nodes s_i , high accuracy of results is provided, allowing a peak-shaped apex formation to be described as W grows (Fig. 2). A close-up view of such an apex is shown in Fig. 2-e. Its curvature 1491 times exceeds that of a spherical drop at $W=0$. It is interesting that more than the half of the nodes s_i is concentrated on the depicted fragment of the surface meridian although its length is less than 1/200 of the part of the total meridian length within the domain $z \geq 0$. As the apex is approached, a monotonic increase of the curvature is accompanied by decreasing the steps $h_i = s_i - s_{i-1}$. So, at $W=4800$ a minimum step attains a value of $h_1 = 8 \cdot 10^{-7}$ and a maximum one, $h_N = 0.06$.

For the scheme A , the limiting values of the magnetic parameter for it have proved to be much lower: $W \approx 60$ (uniform grid) and $W \approx 150$ (adaptive grid). Note that the stabilizing properties of the scheme A modified to be realized on adaptive grids are essentially improved by coordinate-wise relaxation: in [6], due to coordinate-wise relaxation a solution was obtained within $W \leq 750$. However, in the case of the scheme T this procedure did not yield a positive result.

REFERENCES

1. A. D. Myshkis, V. G. Babskii, N. D. Kopachevskii, L. A. Slobozhanin, and A. D. Tyuptsov, *Low-Gravity Fluid Mechanics. Mathematical Theory of Capillary Phenomena*, Springer-Verlag, Berlin etc., 1987.
2. A. D. Myshkis, V. G. Babskii, M. Yu. Zhukov, N. D. Kopachevskii, L. A. Slobozhanin, and A. D. Tyuptsov, *Methods of Solving Hydrodynamic Problems for Low-Gravity Conditions* (in Russian), Naukova Dumka, Kiev, 1992.

3. B. M. Berkovsky and V. K. Polevikov, Numerical Simulation of the Disintegration of Simply Connected Axisymmetric Shapes of a Magnetic Fluid, *Magnit. Gidrodinam.*, no. 4, pp. 60—66, 1983.
4. V. G. Bashtovoi, A. M. Budnik, V. K. Polevikov, and A. G. Reks, Investigation of Doubly-Connected Equilibrium Magnetic Fluid Shapes in Magnetic Field of a Vertical Conductor, *Magnit. Gidrodinam.*, no. 2, pp. 47—53, 1984.
5. V. K. Polevikov and V. M. Denisenko, Numerical Investigation of Equilibrium Shapes of a Drop Rotating in a Gravity Field, *Vestn. Belorus. Univ.*, Ser. 1, Fiz., Mat., Mekh., no. 2, pp. 37—41, 1985.
6. V. K. Polevikov, Application of Adaptive Grids in Calculating a Free Surface in Problems of Magnetic Fluid Statics, *Differents. Uravneniya*, vol. 30, no. 12, pp. 2146—2152, 1994.
7. R. Finn, *Equilibrium Capillary Surfaces*, Springer-Verlag, New York, , 1986.
8. B. M. Berkovsky, V. F. Medvedev, and M. S. Krakov, *Magnetic Fluids* (in Russian), Khimiya, Moscow, 1989.
9. E. Blums, M. M. Mayorov, and A. Cebers, *Magnetic Fluids* (in Russian), Zinatne, Riga, 1989.
10. A. M. Budnik and V. K. Polevikov, Axially Symmetric Equilibrium Shapes of a Fluid in a Toroidal Vessel under Zero-Gravity Conditions, *Izv. Akademii Nauk SSSR — Mekh. Zhidkosti i Gaza*, no. 6, pp. 154—156, 1986.
11. A. N. Vislovich and V. K. Polevikov, Effect of Centrifugal and Capillary Forces on the Shape of the Free Surface of a Magnetic-Fluid Seal, *Magnit. Gidrodinam.*, no. 1, pp. 77—86, 1994.
12. A. N. Vislovich and V. K. Polevikov, Concerning Numerical Simulation of the Failure of a Magnetic-Fluid Seal with a Rotary Outer Profiled Cylinder, *J. Engineering Physics and Thermophysics*, vol. 70, no. 1, 1997.
13. V. K. Polevikov, Stability of a Static Magnetic-Fluid Seal under the Action of an External Pressure Drop, *Fluid Dynamics*, vol. 32, no. 3, pp. 457—461, 1997.

Indices of convergence rate and stability of iteration schemes
for Problem 2 at $h = 1 / 100$

[illegible]

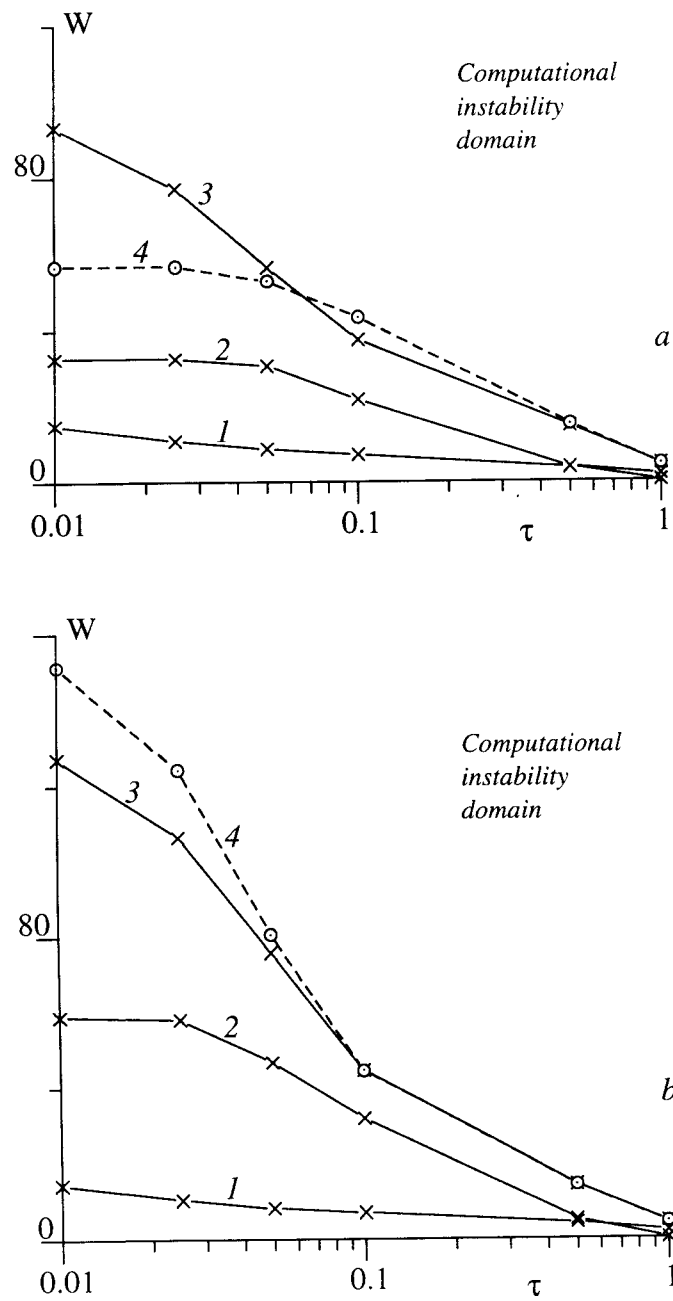


Fig. 1. Boundaries of computational stability of iteration schemes for Problem 2 at $h = 1/20$ (a) and $h = 1/100$ (b): 1, scheme B; 2, scheme A; 3, scheme T-2; 4, scheme T.

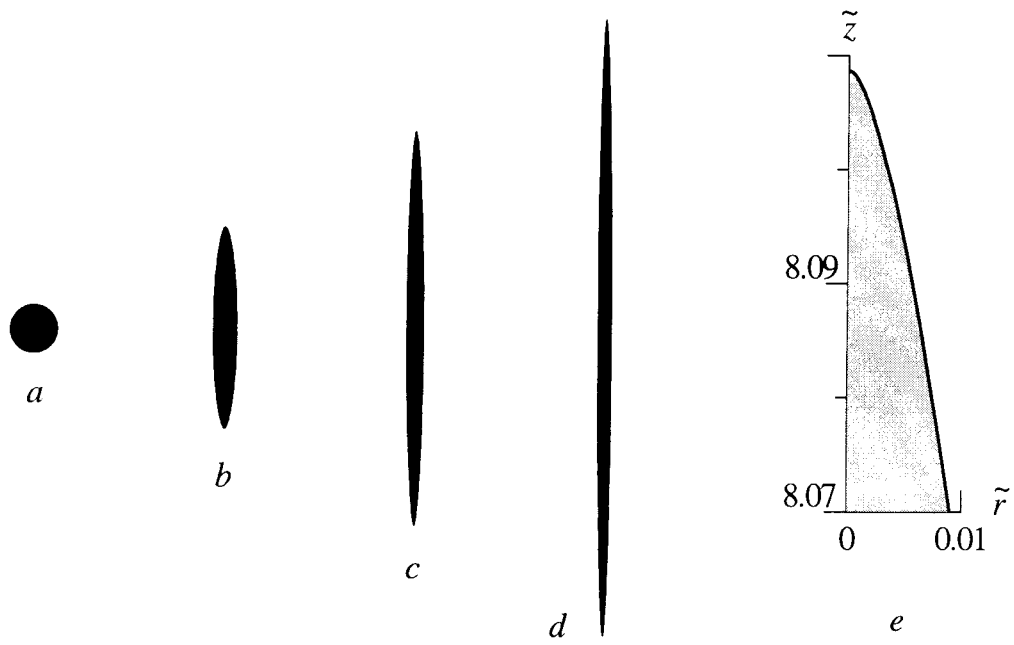


Fig. 2. Drop deformation due to increasing magnetic parameter W : a , $W = 0$; b , 100; c , 1000; d , 4800; e , peak-shaped apex of a drop at $W = 4800$. Problem 2.